Proceedings of ERAD 2006

Areal homogeneity of Z-R-relations

Gerhard Peters, Bernd Fischer, Marco Clemens

University of Hamburg, Hamburg (Germany).

1 Introduction

A standard procedure for quantitative rain measurements by radar is to apply $R(Z)$-relations that are typical for certain geographic areas, and/or seasons. These specific $R(Z)$-relations are usually established on the basis of climatologies of rain gauge data versus simultaneous radar reflectivities (e.g. Michelson and. Koistinen, 2000). Lee and Zawadzki (2006) demonstrated that distrometer-based radar calibration providing the actual $R(Z)$-relation via the the drop size distribution has the potential to eliminate important calibration uncertainties. The benefit of dynamic $R(Z)$-relations based on local distrometer measurements depends on the representativeness of such measurements in space and time. Already Doelling et al. (1998) suspected the existence of coherent time intervals t_m, during which $R(Z)$ is fairly well defined and significantly different from $R(Z)$-relations outside of t_m. Although the nature of such modes and the physical processes behind it are not yet understood, we investigate here the question, if such modes could be exploited to further improve radar based rainfall estimates. The observation by Clemens et al. (2006) that modes seem to be a general phenomenon rather than an exception suggests that such improvements could be eventually relevant even in operational applications. Clemens et al. (2006) also found that the lifetime of modes spans from fractions of a shower duration (minutes) to several hours. In a first step we consider here only "long term modes" whose lifetime suggests that they are related to some mesoscale atmospheric parameters, and show therefore corresponding spatial extensions. In that case local distrometer measurements could be used to establish mode-specific $R(Z)$-relations in real time or near real time which would be applicable in extended areas surrounding the distrometer site.

2 Experimental set up

We used commercial micro rain radars (MRR, METEK) which derive rain drop size distributions RDSDs from the Doppler spectra of rain echoes at vertical incidence (Atlas et al., 1973). Due to the range resolution of the MRR a sampling volume coincident with the measuring height of a weather radar can be chosen, thus avoiding possible biases due to vertical gradients of $R(Z)$. In addition, the large sampling volume of the MRR allows short averaging times, a useful feature, particularly for future real-time applications. System and operating of the MRR parameters are given in Table 1.

Table 1: MRR Parameters

Transmit frequency	24.1 GHz
Doppler resolution	0.191 ms^{-1}
Range resolution	100 m
Height Range	300 m - 3000m
Beam width (3 dB one way)	1 °
Sampling rate (Doppler spectra)	25 s^{-1}
Averaging time	14 s
Measuring cycle time	$\Delta t_{MRR} = 20$ s

13 MRRs were operated for 2 months during the LAUNCH-2005 campaign along a line of 6 km length close to the Meteorological Observatory Lindenberg, Germany. The set-up was supplemented by a small X-band radar (WRDR), which was sited at 3.5 to 6 km distance from the MRRs and was scanning at a fixed elevation angle of 11,3°. The WRDR is based on a commercial nautical radar (FR7112, FURUNO). The original fan beam antenna was replaced by a pencil beam antenna and the logarithmic video amplifier output was fed into a dedicated DSP unit, where after linearization mean powers for each radar pixel are calculated. System and operating parameters of the WRDR are given in table 2.

Table 2: WRDR Parameters

Transmit frequency	9.41 GHz
Sampling rate	10 MHz
Range resolution	15 m
Beam width (3 dB one way)	2.5 °
Beam elevation	11.3°
Pulse repetition rate	2100 s^{-1}
Scanning rate	144 $°s^{-1}$
Pixel size (range × azimuth)	60 m × 2°
Averaging time = measuring cycle time	$\Delta t_{WRDR} = 30$ s
Samples per pixel and averaging time	1400

Correspondence to: Gerhard Peters

gerhard.peters@zmaw.de

3 Calibration of radar-constants

The radar-constants of all radars involved in this experiment were calibrated in three steps:

3.1 Rain gauge $\Rightarrow$ MRR_{ref}

At one of the 13 MRRs sites auxiliary rain gauges were operated. For calibration of this MRR_{ref}, rain events spanning several hours were selected. Periods with high wind speed were discarded to keep rain gauge errors small.

The MRR rain fall RF is calculated from the RDSD $N(D)$ and the terminal fall velocity $v(D)$ by

$$RF = \rho_w \frac{\pi}{6} \Delta t_{MRR} \sum_{\text{rain events}} \left(\int_{\text{drop diameter } D} N(D) v(D) D^3 dD \right) \quad (1)$$

Using a first-guess radar-constant C_0 yields a first-guess RDSD $N_0(D)$ and RF_0. A new radar-constant C_1 was derived by comparison of the first-guess rain fall RF_0 with the gauge measured rain fall RF_g

$$C_1 = C_0 \frac{RF_0}{RF_g} \quad (2)$$

C_1 was used to derive a new RDSD $N_1(D)$, which yields R_1 by insertion in Eq. 1. If micro-wave attenuation can be neglected, the calibration procedure is finished. In this case $N_1(D) = (C_0 / C_1) N_0(D)$ and $RF_1 = (C_0 / C_1) RF_0 = RF_g$ holds. If attenuation is significant, the procedure is to be iterated according:

$$C_i = C_{i-1} \frac{RF_{i-1}}{RF_g} \quad (3)$$

yielding $N_i(D)$ and RF_i. The iteration could be terminated for $i = 2$ already as the selected MRR measuring height was 300 m, where attenuation was small for all occurring rain rates.

3.2 MRR_{ref} $\Rightarrow$ WRDR

RDSDs were measured with MRR_{ref} in a common volume with the WRDR and converted into (Rayleigh) radar reflectivity factors Z_{ref} according

$$Z_{ref} = \int N(D) D^6 dD \quad (4)$$

The WRDR radar-constant was found by regression of $\log Z_{WRDR}$ versus $\log Z_{ref}$

3.3 WRDR $\Rightarrow$ all other MRR

In each common WRDR/MRR volume a first guess MRR radar-constant C_0 was used to create a new MRR radar-constant C_1 according Eq. 5. Z_0 was calculated using Eq. 4 with a first guess RDSD $N_0(D)$.

$$C_1 = C_0 \frac{Z_0}{Z_{WRDR}} \quad (5)$$

As the heights of the common volumes were between 700 and 1200 m, micro-wave attenuation was sometimes significant for the MRR. Therefore the procedure had to be iterated similarly as in 3.1:

$$C_i = C_{i-1} \frac{Z_{i-1}}{Z_{WRDR}}, \quad (5)$$

where Z_{i-1} was calculated with Eq. 4 using N_{i-1}, and N_{i-1} was derived with C_{i-1}.

3.4 Validation

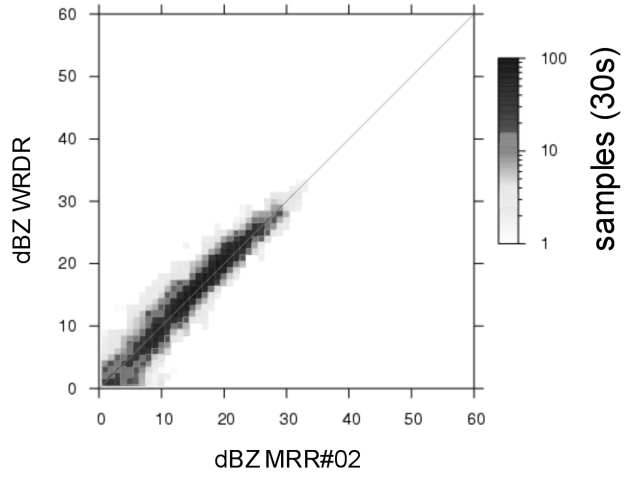

Fig.1. Comparison of radar reflectivity between WRDR and MRR#02

Fig. 1 shows an example of comparisons of Z measurements between WRDR and MRR#02 after calibration for the whole measuring period from 15 September to 25 October 2005. The MRR time series was resampled with 30 s time steps in order to match the WRDR resolution. The regressions look very similar for the 12 other MRRs.

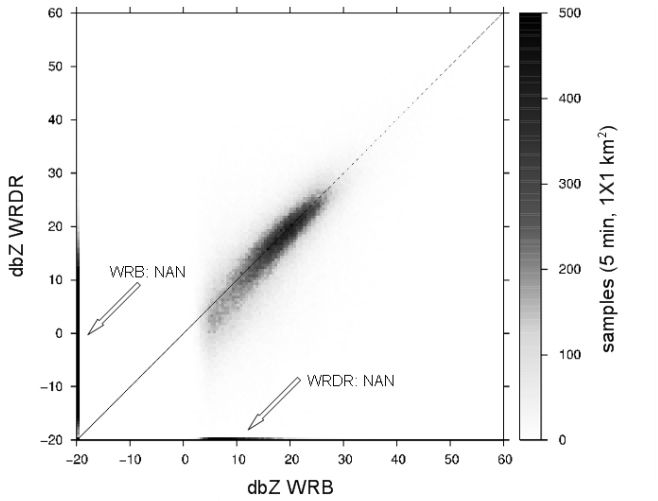

Fig.2. Comparison of radar reflectivity between WRDR and the DWD weather radar Berlin (WRB).

Simultaneous measurements of rain scans of the DWD weather radar Berlin (WRB) at 50 km distance NW from the WRDR were used to cross-check the absolute calibration. The WRB rain scan cycle is 5 min and the data were available in 1×1 km^2 pixels on a Cartesian grid. For comparison WRDR-data were averaged and projected on the same grid in a 16×16 km^2 square centered around the WRDR site. Occasionally only one of both systems provided valid values, while the counter value was flagged invalid (not a number). Such samples were displayed on the respective abscissa and ordinate (labeled WRDR NAN or WRB NAN). For radar reflectivities above 10 dBZ the mean bias between both radars is less than 1 dB.

4 Modes

Fig. 3 shows two subsequent time intervals of several hours duration with significantly different modes. The small-drop mode in the bottom panel would cause an overestimation of rain rate of factor 4, if a $R(Z)$-relation valid for the large-drop mode in the top panel would be used.

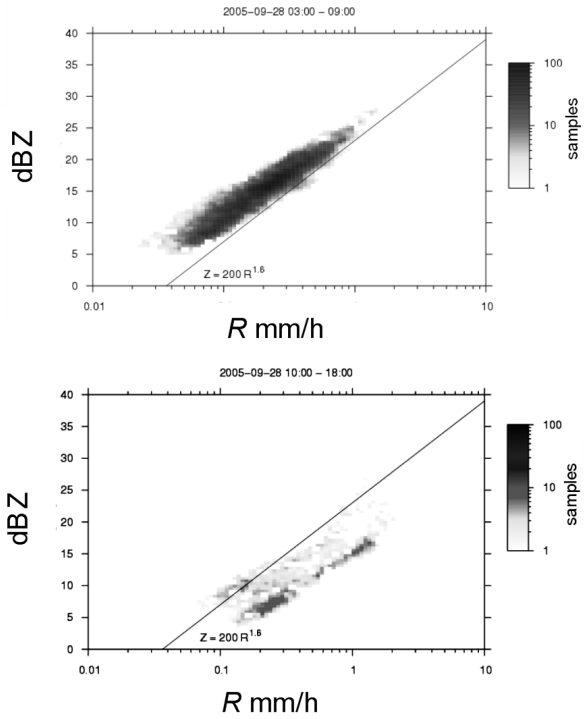

Fig.3. Z versus rain rate RR. The solid lines represent a standard $R(Z)$-relation. Top: 6-hour interval with larger drops. Bottom: Subsequent 8-hour interval with smaller drops.

In Fig. 4 rain rates, as derived from $R(Z)$-relations of the form $Z = aR^b$, are compared with "true" rain rates derived directly from RDSDs. In the top panel (R_f versus R) fixed coefficients, $a = 200$ and $b = 1.6$, were used. In the bottom panel (R_a versus R) a and b were adapted according to subjectively identified modes. All rain data during the whole measuring campaign from 15 September to 25 October were included. The scatter is smaller for the adapted coefficients, which is not surprising, because the "training" data for generating the adapted coefficients and the "validation" data are identical (here data of MRR#02).

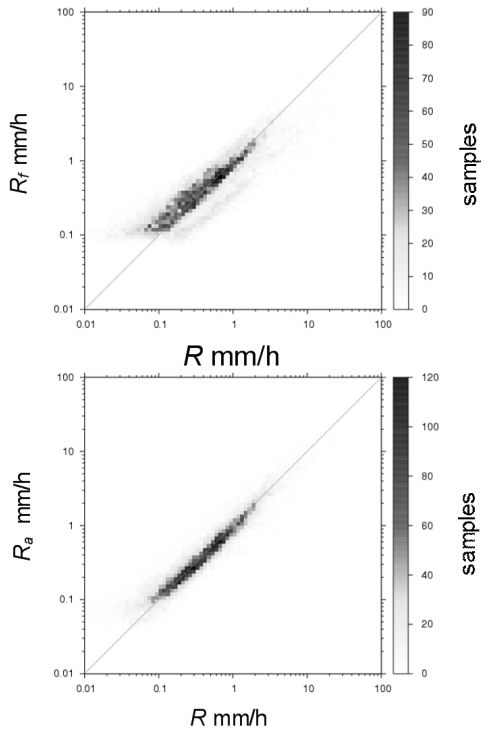

Fig.4. Rain rate at MRR#2-site derived from R(Z) relation of the form Z = aRb versus rain rate derived from RDSD. Top: Rf using fixed coefficients a =200, b = 1.6. Bottom: Ra, derived with adapted coefficients. Adaptation using MRR#2 data.

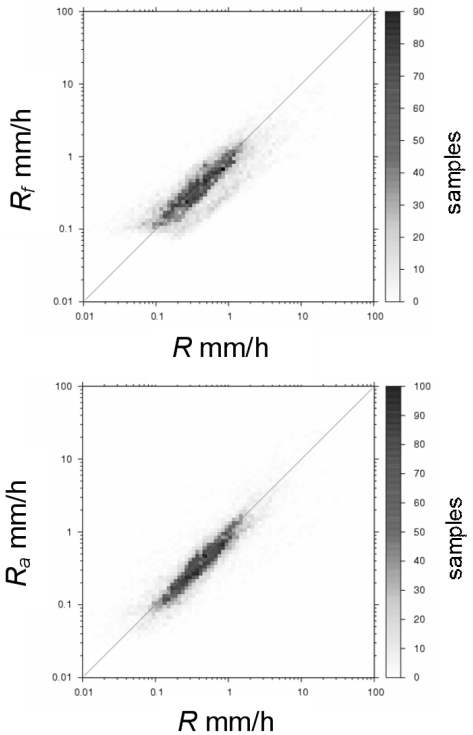

Fig.5. Same as Fig.4, but at MRR#15-site. Adaptation using again MRR#2 data.

The usefulness of adapted coefficients for areal rain measurements depends on whether or not adapted coefficients lead to improved agreement also for measurements in some distance from the "training" site. Therefore, $R(Z)$-relations, which were adapted with MRR#02-data were applied to data of MRR#15 at 6 km distance from MRR#02, see Fig.5. One recognizes in Fig.5 also a significant reduction of scatter after application of the adapted coefficients. Particularly the extreme errors appearing in R_f are efficiently removed in R_a.

5 Summary and outlook

The habit of rain fall to display modes of $R(Z)$-relations that seem to be stable in the order of hours has been utilized to generate locally mode-specific $R(Z)$-relations $R(Z)_a$ on the basis of distrometer measurements (MRR). Application of $R(Z)_a$ to radar reflectivities, measured in 6 km horizontal distance, yielded rain rates R_a that deviate significantly less from distrometer rain rates R than rain rates R_f obtained with a fixed $R(Z)$-relation. It should be noted that the reduced scatter of rain rates refers to time averages of only 20s. On this time scale the distance of 6 km is far beyond the correlation-distance of the rain field (not shown here).

In this first attempt the data were analyzed off-line and the identification of modes and the estimation of their persistence were made on a subjective basis. Nevertheless, we believe that there are good prospects for an automatic near-real-time procedure; because the method seems to be particularly useful during periods with strong anomalies (extreme errors were efficiently eliminated). These situations are principally easier to detect than "near normal" conditions. So far no other classification of rain events has been made. We expect that the analysis of 4-dimensional radar reflectivity fields will provide further hints on the areas where locally determined $R(Z)_a$-relations are applicable. The search of such indicators is underway within the ongoing project AQUARADAR (Simmer, 2006). Further we did not yet exploit the possibility to analyze profiles of RDSDs. The profile information accompanied with a better physical understanding of the nature of modes (Clemens, 2006) may also allow improved estimates of the areal extension and persistence of modes in the future.

Acknowledgements: The work is supported by DFG project AQUARADAR. We thank Hans Münster from MPI-Hamburg for his great support in preparing and setting up the radar instrumentation. The reflectivity data of the Berlin weather radar were kindly provided by Jörg Seltmann/DWD.

References

Atlas, D., R.C. Srivastava and R.S. Sekhon, 1973: Doppler radar characteristcs of precipitation at vertical incidence, *Rev. Geophys. Space Phys.,* **11**, 1-35.

Clemens, M, G. Peters, P. Winkler, 2006: Concepts of spectrral and integral modes in measured raindrop size distributions, ERAD 2006, this proceedings volume.

Doelling, I.G. J. Joss and J. Riedl, 1998: Systematic variations of *Z–R*-relationships from drop size distributions measured in northern Germany during seven years, *Atmos. Res.,* **47-48**, pp. 635-649.

Lee, G.W. and I. Zawadzki, 2006, Radar calibration by gage, disdrometer, and polarimetry: Theoretical limit caused by the variability of drop size distribution and application to fast scanning operational radar data, *Journal of Hydrology,* In Press, Available online 17 February 2006

Michelson, D. B., J. Koistinen, 2000: Gauge-Radar Network Adjustment for the Baltic Sea Experiment, *Phys. Chem. Earth (B)*, **25**, pp. 915-920